Computational Analysis of Gas Turbine Preswirl System Operation Characteristics

M. CAGAN
Computer Aided Engineering
Otokar Otobus Karoseri A.S.
Ataturk Cad. No: 9, Arifiye TR-54580 Sakarya
TURKEY
mcagan@otokar.com.tr

A. C. BENIM
Department of Mechanical and Process Engineering
Duesseldorf University of Applied Sciences
Josef-Gockeln-Str. 9, D-40474 Duesseldorf
GERMANY
alicemal.benim@fh-duesseldorf.de

D. GUNES
Department of Mechanical Engineering
Istanbul Technical University
Inonu Cad. No: 87, Gumussuyu TR-34437 Istanbul
TURKEY
gunes@itu.edu.tr

Abstract: - Gas turbine engine efficiency can be increased by the improvements of the cooling air system. In this study, gas turbine preswirl cooling system is computationally analyzed using a validated three-dimensional quasi-steady model. In the first phase of the study, the system is analyzed with respect to different operating conditions, for understanding its behavior. In this part, the dependence of the discharge coefficient and the temperature drop on the inverse of the swirl ratio parameter are employed to characterize the system. In the second phase of the analysis, the possibilities of improving the system performance is investigated by implementing different modifications on the system geometry.

Key-Words: - Gas turbine cooling, Preswirl system, Discharge coefficient, Performance, CFD.

1 Introduction

In many industrial gas turbines, a preswirl system is used for supplying the cooling air to turbine blades for increasing the performance and extending the life of the engine. In preswirl systems the cooling air is expanded through nozzles located on stator component and collected by receiver holes located on rotor component. Using appropriately inclined nozzles the necessary amount of swirl in the rotation direction of the rotor disc is generated. Thus, the pressure losses in the preswirl chamber (wheel space) are minimized and the total temperature in the rotating frame of reference is reduced before cooling the rotor blades.

Since gas turbine engine efficiency depends strongly on the performance of the cooling air system, a detailed understanding of the fluid mechanics and heat transfer processes in cooling air systems is essential. Therefore, it has been one of the main research themes of many computational studies. Fundamentals of internal cooling-air systems of gas turbines have already been investigated [1,2]. The first study on preswirl systems was carried out experimentally by Meierhofer and Franklin [3]. In that study, they showed that the system performance can be identified by using the ratio of the real velocity to the isentropic velocity (C/C_{is}) at the preswirl nozzle exit. Since 1990's the computational Fluid Dynamics (CFD) methods have achieved such a level of maturity that, researchers have started to apply CFD for the investigation of even very complex flow structures that typically occur in turbomachinery [4-6]. Early computational studies on preswirl systems were performed for simplified axisymmetrical arrangements [7,8]. In a three-dimensional study [9], the preswirl nozzle was not included in the solution domain and the orifice geometries of the receivers were simplified as

having square cross-sections, and the annular domain was treated as a planar system. Another three-dimensional study was carried out with a more realistic arrangement [10], where, however, the receiver hole was modeled as circumferential slot. Some realistic three-dimensional computational studies [11,13] were performed by modeling the rotor-stator interaction by using quasi-steady formulation. The rotor-stator interaction for the modeling of such systems has computationally been investigated using two-dimensional arrangements [14]. In that study [14], it was found out that the validity of the quasi-steady modeling depends on the inverse of the ideal swirl ratio ($1/\beta_{id}$) parameter. However, that study [14] was not extended to three-dimensional cases, and the investigation was not performed for how the performance of the system is influenced according to different operating conditions and geometrical parameters. This aspect is the main emphasis of the present study: A preswirl system has been analyzed, using a three-dimensional validated computational model, for different operating conditions and geometrical modifications.

2 Modeling

General purpose CFD code Fluent 6.3 [15], which employs finite volume formulation, has been used for analyzing the system. The flow has been modeled as compressible and turbulent flow through a three dimensional configuration. Pressure-correction algorithm SIMPLEC [16] has been employed for treating the velocity-pressure coupling. The realizable version of high Reynolds number k-ε model [17] has been utilized as the turbulence model. On solid surfaces, no-slip conditions apply for the momentum equations, in conjunction with a non-equilibrium wall-functions approach [18]. An adiabatic wall has been assumed for the energy equation. At the inlet, the total pressure and the total temperature have been applied as boundary conditions, whereas the static pressure has been prescribed at the outlet boundary. For the discretizaton of the convection terms, a second order upwind discretization scheme [19] has been used for the equations of all convective-diffusively transported variables.

Due to expected flow periodicity in circumferential direction, just a representative pitch has been included into the solution domain restricting by periodic boundaries. Furthermore, not whole the radial extents of the discs have been modeled, but only a section in the vicinity of the nozzle and the receiver has been included into the domain. In Fig.1 the modeled computational domain and the applied boundary conditions are illustrated.

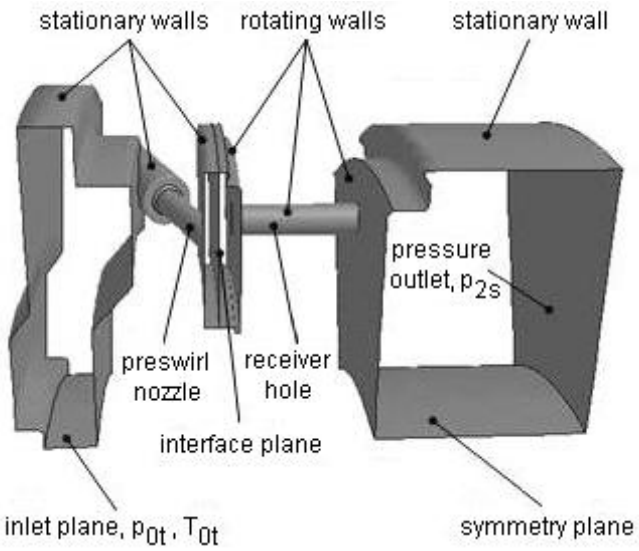

Fig.1. Computational domain and boundary types

An unstructured tetrahedral grid has been generated on the computational domain. For the near-wall cells, special attention has been paid to obtain appropriate non-dimensional wall distance values (y^+), within a range of $30<y^+<100$ [15,20], by means of local grid adaptations. Grid independent results have been ensured by testing different grids consisting of different number of cells and resolutions, at the beginning of the investigation. The final grid, which was employed in the computations, has been generated with approximately 400,000 cells.

In stator-rotor systems, the modeling of the interface, i.e. the handling of relative motion between the stationary and rotating parts is very important. For the present investigation, the frozen rotor model has been employed considering the flow in both stationary and rotating sub-domains as steady-state problems. While using the quasi-steady modeling, the flow has been computed for six relative positions of rotor with respect to stator for increasing the accuracy of the results. Thus, the quasi-steady results have been obtained by averaging the results of the six quasi-steady computations.

3 Validation

The computational model has been validated using the measurements, which performed at the test rig of the Institute for Thermal Turbomachinery of University of Karlsruhe, Germany [21,22]

The flow through the system is simulated for different operating conditions, i.e. for different pressure ratios (Π) and for different rotor rotational speeds (N). In this investigation, the parameters of pressure ratio and swirl ratio have generally been used in order to characterize the different operating conditions. Pressure ratio (Π) is the ratio of inlet total pressure (p_{0t}) to the outlet static (p_{2s}) pressure, and swirl ratio (β) is the ratio of flow

absolute tangential velocity (C_t) to the local rotor circumferential velocity (U).

$$\Pi = \frac{p_{0t}}{p_{2s}} \tag{1}$$

$$\beta = \frac{C_t}{U} \tag{2}$$

Ideal swirl ratio (β_{id}) is defined replacing flow tangential velocity (C_t) with ideal flow tangential velocity ($C_{t,id}$) in Eq.2. The ideal tangential velocity is obtained by using Eq.4 assuming isentropic expansion through the preswirl nozzle, and no change between the preswirl nozzle exit and the receiver inlet.

$$\beta_{id} = \frac{C_{t,id}}{U} \tag{3}$$

$$C_{1t,id} = \sqrt{\frac{2\kappa}{\kappa-1} RT_{0t}\left(1-\left(\frac{p_{1s}}{p_{0t}}\right)^{\frac{\kappa-1}{\kappa}}\right)}\cos\alpha \tag{4}$$

The schematic view of the preswirl system and the other velocity components occured within the system is shown in Fig. 2 [21]. The mathematical definitions of relative velocities W_{1t} and $W_{2ax,id}$ are given in Eq.5 and Eq.6 respectively [23].

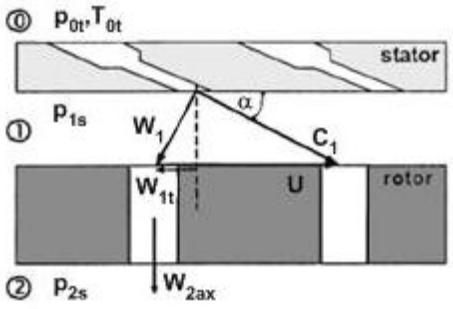

Fig.2: The schematic view of the preswirl system and the velocity components [21]

$$W_{1t,id} = U - C_{1t,id} \tag{5}$$

$$W_{2ax,id} = \sqrt{\frac{2\kappa}{\kappa-1} RT_{1trel}\left(1-\left(\frac{p_{2s}}{p_{1trel}}\right)^{\frac{\kappa-1}{\kappa}}\right)} \tag{6}$$

The amount and the temperature of the flow leaving the system are important variables in the assessment of the performance of preswirl systems. The parameter of system discharge coefficient (C_D) is described as the ratio of the real mass flow rate to the ideal mass flow rate through the system [21]. The discharge coefficient can also be defined for each component, namely for preswirl nozzles ($C_{D,PSN}$) and for receivers ($C_{D,R}$). The mathematical definitions of discharge coefficients for the system, preswirl nozzles and receivers are given respectively [21], as below.

$$C_D = \frac{\dot{m}_{real}}{\frac{A_{PSN}\,p_{0t}}{\sqrt{RT_{0t}}}\sqrt{\frac{2\kappa}{\kappa-1}\left[\left(\frac{p_{2s}}{p_{0t}}\right)^{\frac{2}{\kappa}}-\left(\frac{p_{2s}}{p_{0t}}\right)^{\frac{\kappa+1}{\kappa}}\right]}} \tag{7}$$

$$C_{D,PSN} = \frac{\dot{m}_{real}}{\frac{A_{PSN}\,p_{0t}}{\sqrt{RT_{0t}}}\sqrt{\frac{2\kappa}{\kappa-1}\left[\left(\frac{p_{1s}}{p_{0t}}\right)^{\frac{2}{\kappa}}-\left(\frac{p_{1s}}{p_{0t}}\right)^{\frac{\kappa+1}{\kappa}}\right]}} \tag{8}$$

$$C_{D,R} = \frac{\dot{m}_{real}}{\frac{A_{R}\,p_{1trel}}{\sqrt{RT_{1trel}}}\sqrt{\frac{2\kappa}{\kappa-1}\left[\left(\frac{p_{2s}}{p_{1trel}}\right)^{\frac{2}{\kappa}}-\left(\frac{p_{2s}}{p_{1trel}}\right)^{\frac{\kappa+1}{\kappa}}\right]}} \tag{9}$$

The variation of computational and experimental [21] values of the discharge coefficients obtained for preswirl nozzles, for receivers and for the system is shown in Fig.3, Fig.4 and Fig.5 respectively. Both Experiments and computations are indicated by symbols, the solid line in the figure shows the variation of the inverse of ideal swirl ratio ($1/\beta_{id}$).

It has been observed that preswirl nozzle discharge coefficients ($C_{D,PSN}$) could be predicted quantitatively very well for a broad range of operating conditions. The computed receiver discharge coefficients ($C_{D,R}$) show a very good qualitative agreement with the mesasurements. However, there are slight deviations between the computed and the measured values. This might be due to the fact that the approximated solutions of the frozen rotor model deviates from the that of sliding mesh technique, i.e. transient model. This might deteriorate the predicted receiver discharge coefficients rather than the predicted preswirl nozzle discharge coefficients, because the receivers are located in the rotating sub-domain.

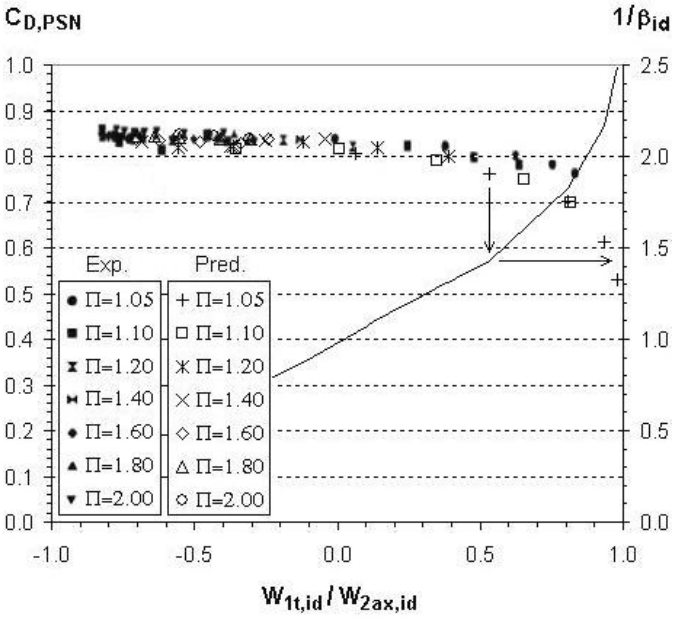

Fig. 3: Preswirl nozzle discharge coefficient (arrows show how to find the $1/\beta_{id}$ value for a test case)

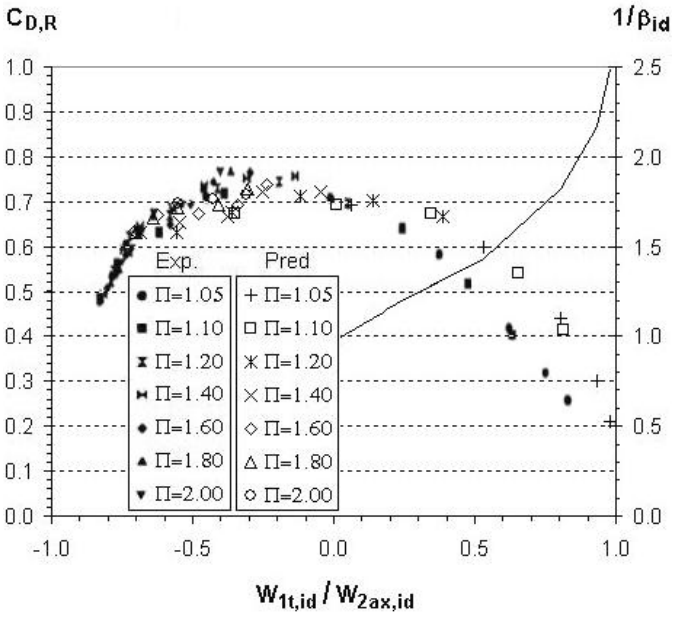

Fig. 4. Receiver discharge coefficient

For the whole system, the discharge coefficient (C_D) exihibits fairly good agreement with the measurements quantitatively for a broad range of operating conditions. However, it should be noted that the deviations between the computations and the measurements increase for high velocity ratios, and this indicates that the computational model cannot predict the measurements well for high values of inverse of ideal swirl ratio ($1/\beta_{id}$). Especially, the validity of the computational model fails for $1/\beta_{id}$ >1.25, which corresponds to $1/\beta$ >1.5. This finding confirms the results of the previous two-dimensional study of Benim et al.[14], where it was proposed that the quasi-steady formulation to be valid for the range $1/\beta_{id}$ <1.5. However, in that study [14] they compared the quasi-steady results with the unsteady results (for two-dimensional cases), whereas in the present investigation the three-dimensional quasi-steady results have been compared with the measurements. That is why here the validity limit decreases to the value $1/\beta_{id}$ =1.25, in the present case.

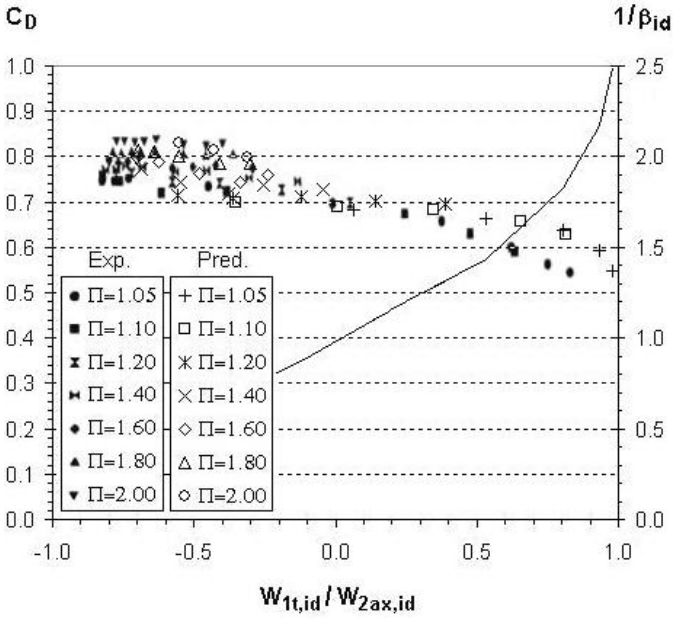

Fig.5. System discharge coefficient

The temperature drop of the cooling air between the inlet of the system and the outlet of the receiver holes is displayed for the computed and the measured [22] values in Fig.6. It is observed that computational model can predict the temperature drop values qualitatively very well. It should be noted that the wall boundaries of the system were assumed to be adiabatic, and this might be causing lower computed temperature values than measurements. However, the test rig does not have necessarily to be an adibatic system, because the frictional heating at the labyrinth seal might be transferred to the flow through the solid rotor disc by heat conduction.

In a three-dimensional study of Benim et al. [13], it was shown that the cooling air temperature predictions could be improved either extending the computational model into the conjugate heat transfer problem with solid rotor disc or correcting the measurements by compensating the heating of the fluid. Similarly, in the present investigation the computed cooling air temperature drop across the system can be quantitatively improved using those approaches.

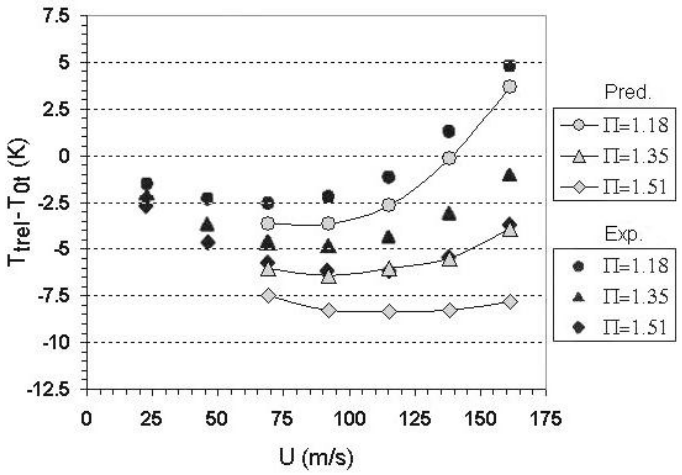

Fig.6. Temperature drop across the system

4 Results

4.1 Different Operating Conditions

Using the validated computational model, operation characteristics and the performance of the system have been investigated with respect to different operating conditions. The incidence angle of the flow towards the receiver holes has a considerable effect on the performance of the system, since it remarkably influences the behavior of the flow. This can be analyzed using the inverse of the swirl ratio ($1/\beta$) parameter. For different rotor speeds, the axial velocity distributions (normalized by the maximum value occurring in this plane, for all of the cases) are illustrated in Fig.7 on a radial plane which intersects the receiver holes (blank areas indicate the regions with negative axial velocity, which are in opposite direction to the main flow).

For the case displayed in Fig.7b the area weighted average of $1/\beta$ at the inlet of receiver holes takes the value of 0.95, which is close to unity. In this case, the tangential velocity of the flow, coming out of the preswirl nozzles is similar to the value of the rotor circumferential velocity. Thus, this case is very close to the operating condition called "nominal swirl", where the swirl number is identically 1.0. In this case near "nominal swirl" the fluid can flow through the receiver holes without any separation from the receiver walls. In Fig.7a the average value of $1/\beta$ is 0.46, which corresponds to the "over swirl" case, whereas in Fig.7c the average value of $1/\beta$ is 1.5, which corresponds to "under swirl" case. In over and under swirl cases the flow towards the receiver holes has inferior incidence angles, which cause flow separation.

The different cases of the flow approaching to the receiver are summarized in Table 1 with respect to swirl ratio (β) parameter at the receiver inlet.

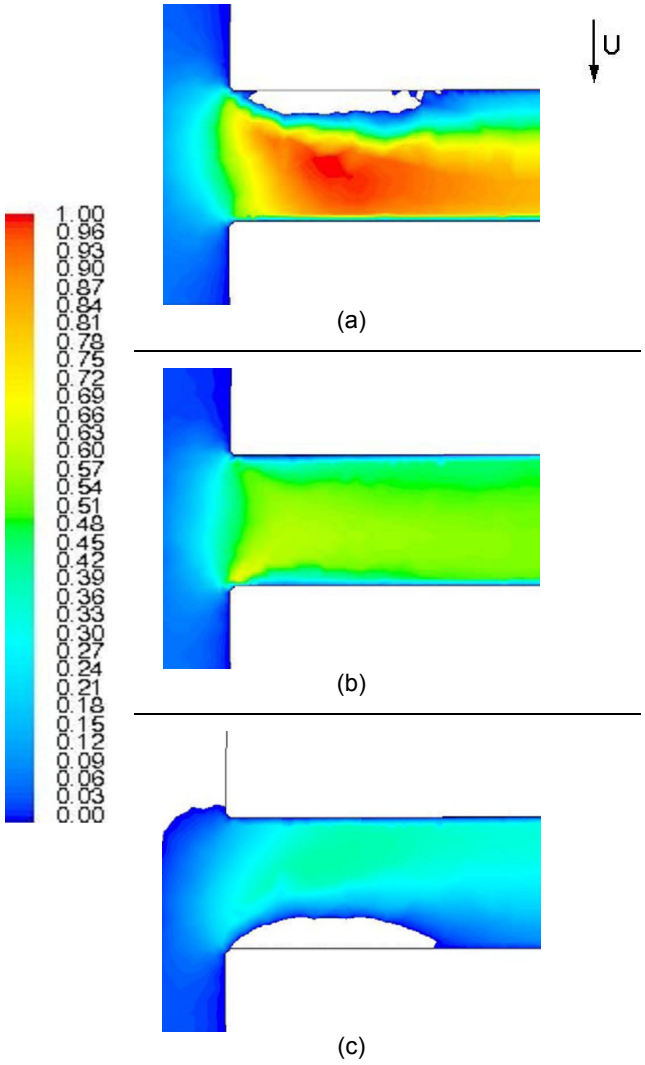

Fig.7. Distribution of axial velocity at the inlet section of receivers; (a) Π=1.8, N=3000 rpm, (b) Π=1.6, N=7000 rpm, (c) Π=1.2, N=6000 rpm

Table 1. Different cases of the flow approaching to the receiver with swirl ratio at the receiver inlet

Over swirl	$\beta > 1$ (or $1/\beta < 1$)
Nominal swirl	$\beta = 1$
Under swirl	$\beta < 1$ (or $1/\beta > 1$)

In Fig.8 the discharge coefficient of receiver holes ($C_{D,R}$) is displayed for various operating conditions. For the operating conditions far away from the nominal swirl case, i.e. for strong over and under swirl cases, the receiver discharge coefficient values decrease substantially, whereas for the operating conditions close to nominal swirl the receiver discharge coefficient exhibits higher values. As mentioned previously, since air separates at the inlet section of the receiver holes for strong over and under swirl operating conditions,

effective cross section of the flow decreases (vena contracta). Therefore, the discharge behavior of the receivers deteriorates for strong over and under swirl cases.

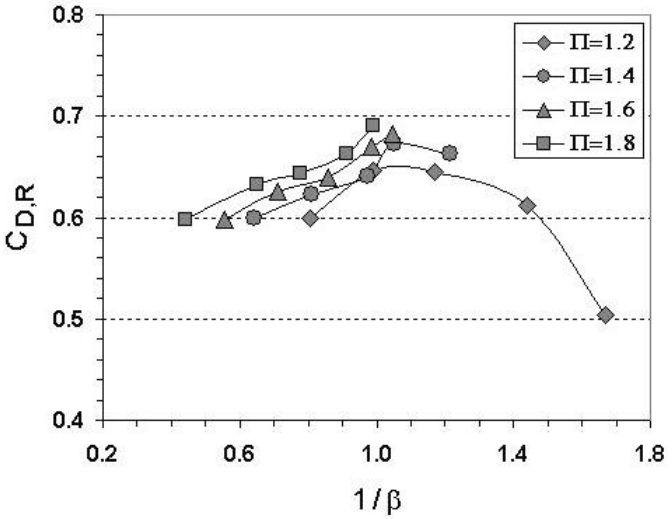

Fig.8. Variation of receiver discharge coefficient

The area weighted average of relative total temperature ($T_{t,rel}$) (normalized by inlet total temperature: T_{0t}) with respect to inverse of swirl ratio ($1/\beta$) parameter is illustrated in Fig.9 for various operating conditions. It has been observed that the pressure drop (Π) across the system has a substantial influence on the cooling air temperature, because the flow tangential velocity at the exit of preswirl nozzle increases with the pressure drop across the preswirl nozzle, and this decreases the temperature of the flow according to Eq.10 [22].

$$T_{trel,id} = T_{0t} + \frac{U^2 - 2UC_{t,id}}{2c_p} \tag{10}$$

Beside the pressure ratio, the rotor rotational speed has also remarkable influence on the cooling air temperature. For the operating conditions in the vicinity of nominal swirl, low cooling air temperatures, i.e. better cooling performance, have been obtained. However, for strong over and under swirl cases, due to flow separations the viscous losses through the system increase, and this causes a temperature increase at the receiver outlets. Thus, the system produces lowest cooling air temperature at nominal swirl condition. Especially, better cooling performance can be obtained by using preswirl systems instead of using conventional systems, because the tangential velocity component of the flow reduces the temperature increase according to Eq.10.

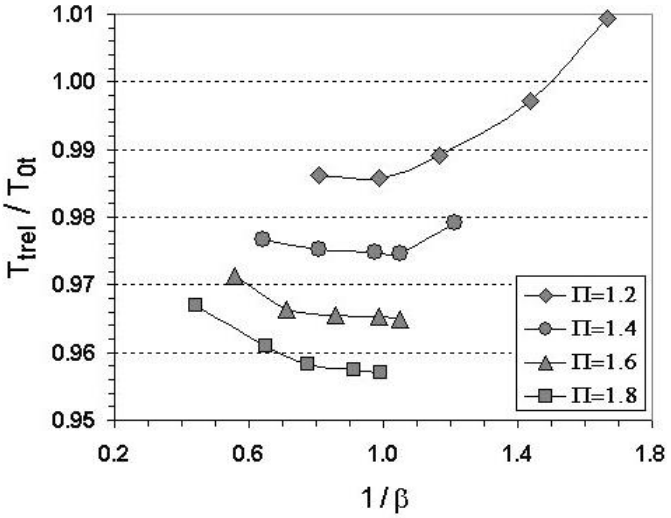

Fig.9. Variation of cooling air temperature at the receiver outlet

4.2 Different Geometrical Modifications

4.2.1 Fillet Radius of Receiver Inlet

In this study, it has been shown that the incidence angle of the flow towards the receivers has a considerable effect on the system performance. Decreasing the losses due to flow separations at the inlet section of the receivers has been investigated using different radiused receiver inlets. Fig.10 and Fig.11 illustrate the variation of the receiver discharge coefficient ($C_{D,R}$) and the variation of the cooling air temperature drop (T_{trel}-T_{0t}) across the system respectively.

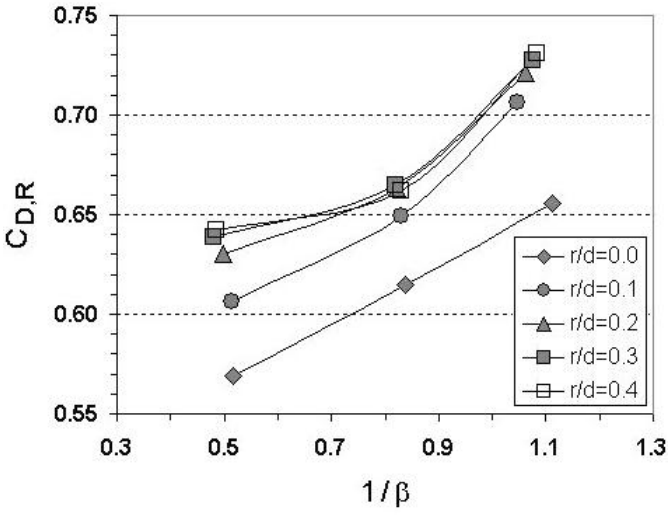

Fig.10. Receiver discharge coefficient with fillet radius

It has been found out that radiusing the fillet of receiver inlets to the value of r/d<0.3 (r: fillet radius of receiver inlet, d: receiver diameter) increases the

receiver discharge coefficient, because radiused inlets decrease the disturbances of the flow at the receiver inlets and the size of the flow separation regions. Therefore, effective cross section of the flow through the holes increases and this improves the discharge behavior of the receivers. Cooling air temperature decreases as well, since the viscous dissipation due to disturbances also decreases through the flow field. However, beyond a certain radiusing value, i.e. r/d>0.3, no further improvement for the performance of the system could be obtained.

In an experimental study, Dittmann et al. [23] showed that discharge coefficients of orifices in rotating discs could be increased by either radiusing or chamfering the orifice inlets, and this finding is in agreement with the results of present computations.

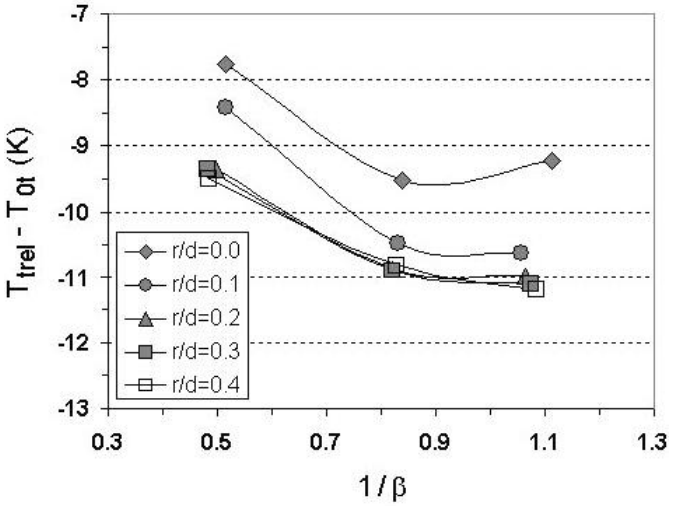

Fig.11. Temperature drop with fillet radius

4.2.2 Receiver Length

The effect of the receiver length (l) on the performance of the system has been investigated using different receiver length sizes. Fig.12 shows the receiver discharge coefficient ($C_{D,R}$) variation with respect to different receiver lengths for different operating conditions. It has been obtained that the shortest receiver has the minimum value of receiver discharge coefficient, because in case of short receiver hole the separated cooling air through the hole leaves the hole without reattaching to the wall. Therefore, the disturbed flow has to leave the system without recovering itself in a chaotic way, and this deteriorates the discharge behavior of the receivers substantially. Due to such disturbances within the flow, the cooling air temperature drop (T_{trel}-T_{0t}) decreases by increasing the viscous losses (Fig.13). Increasing the receiver length increases the discharge of the flow through the holes, because the separated flow at the inlet section of the receivers can reattach to the walls, and in this way the flow regime stabilizes partially before leaving the holes. Therefore, extending the receiver length to a certain value (e.g. l/d=3-4) improves the performance of the system by decreasing the losses. However, with the further increase of the receiver length (i.e. l/d>4) no improvement has been obtained.

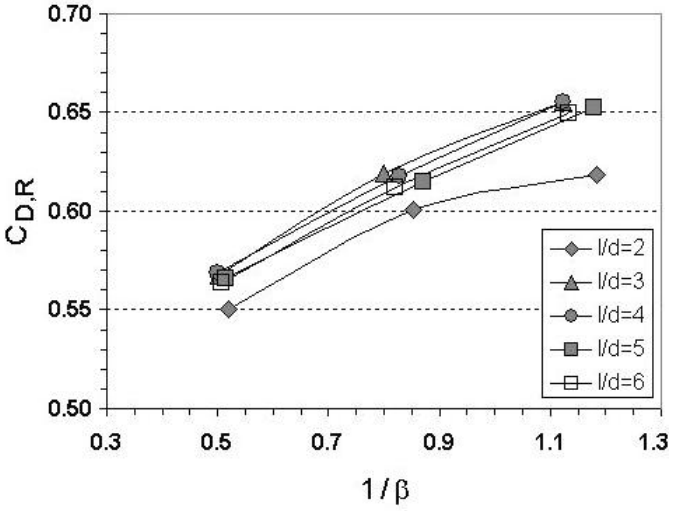

Fig.12. Receiver discharge coefficient with receiver length

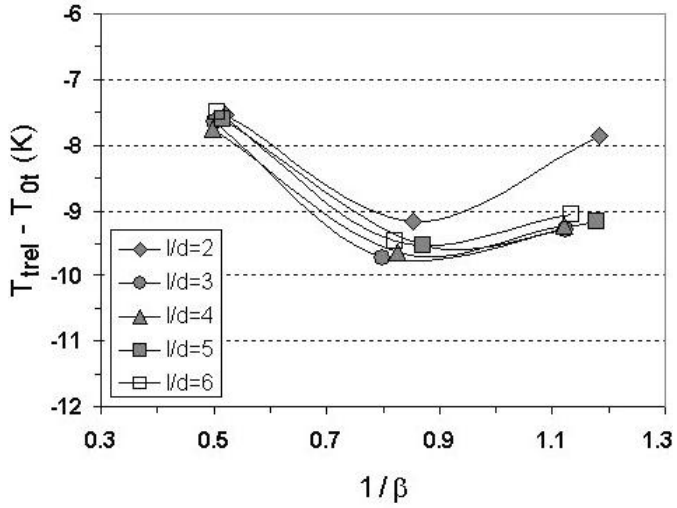

Fig.13. Temperature drop with receiver length

In order to analyze the influence of the length increase better, in Fig.14 the receiver discharge coefficient is shown for only one operating condition against the receiver hole length. It is observed that extending the receivers beyond a certain value decreases slightly the receiver discharge coefficient, because friction losses through the flow increase. This finding confirms the experimental and numerical study of Wittig et al. [24] on rotating discs with orifices. Thus, the flow behaves; in case of short receivers as if it flows through

an orifice, whereas in case of long receivers as if it flows through a pipe.

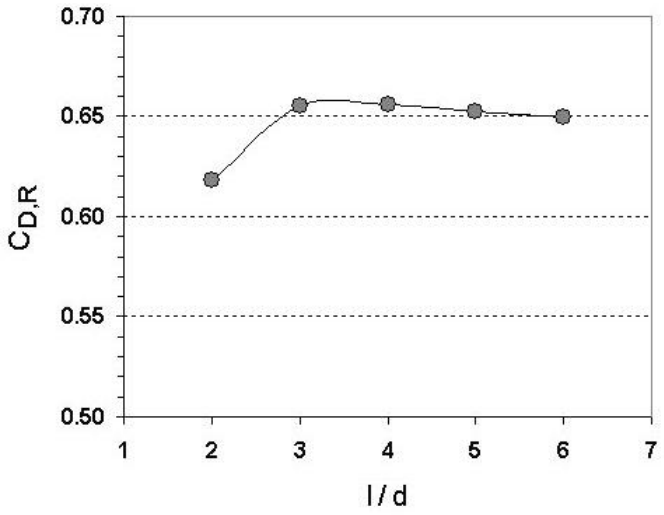

Fig.14. Receiver discharge coefficient with receiver length for one operating condition

4.2.3 Preswirl Chamber Width

The effect of the preswirl chamber width (s) on the system performance has been investigated, and the receiver discharge coefficient ($C_{D,R}$) is displayed in Fig.15 with respect to different chamber width. It has been observed that the receiver discharge coefficient of the geometrical configuration with the minimum chamber width takes minimum values for low rotor rotational speeds. For high rotor rotational speed, i.e. under swirl operating condition, the configuration with the s/d=1.0 value has the maximum receiver discharge coefficient, whereas the other configurations, especially with wider chambers exhibit smaller discharge coefficient values. As a result, for receiver discharge coefficients, in case of over swirl operating conditions no substantial dependence on preswirl chamber width has been observed, whereas in case of high rotor rotational speed (under swirl) operating conditions the receiver discharge coefficient exhibit substantial differences with respect to different chamber width.

For analyzing this substantial differences of the receiver discharge behavior versus chamber width, the losses within the chamber may be investigated with the parameter of effective velocity ratio ($C_t/C_{t,id}$) at the receiver inlet. This velocity ratio variation which represents the deceleration of the flow by rotor disc is shown in Fig.16. It has been observed that for over swirl case the configuration with the narrowest chamber (s/d=0.5) exhibits minimum effective velocity ratio in comparison to the others, because of high velocity gradients. However, for under swirl case the effective velocity ratio increases, due to higher rotor rotational speed. The middle width chambered configurations (s/d=1.0-1.5) exhibit similar preswirl chamber performance, whereas the wide chambered configuration (s/d=2.0) has lower chamber performance. This might be due to the fact that gross amount of fluid mass within the chamber is subjected to recirculation, i.e. a chaotic flow field, and this increases the viscous losses within the flow.

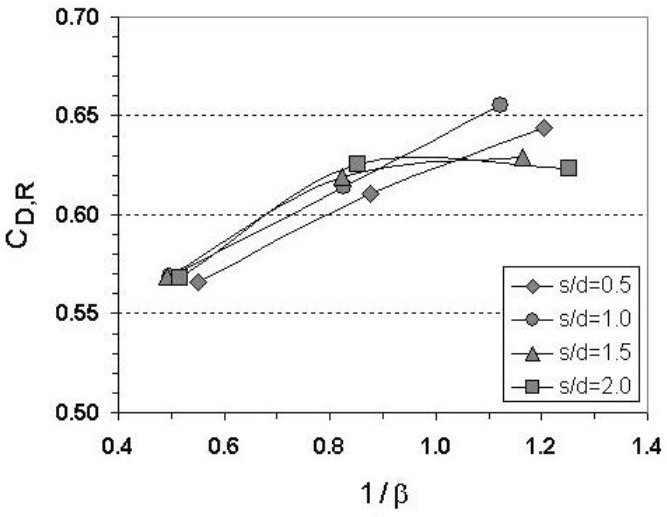

Fig.15. Receiver discharge coefficient with chamber width

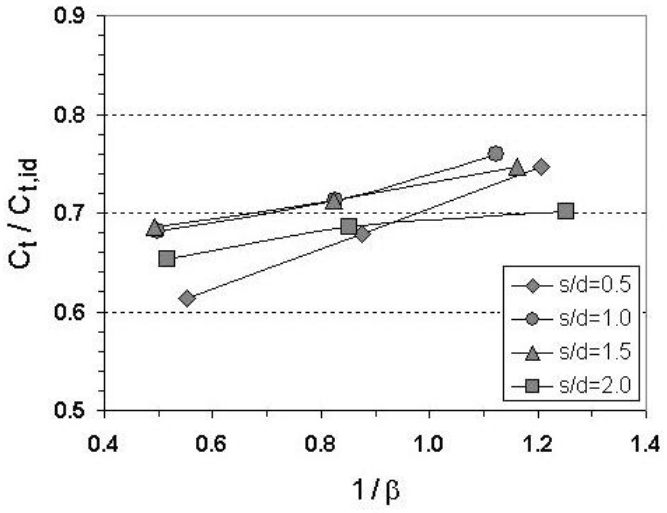

Fig.16. Effective velocity ratio with chamber width

The temperature drop variation (T_{trel}-T_{0t}) across the system with respect to different chamber width is shown in Fig.17. It has been found out that the middle chambered arrangement (s/d=1.0) has the best cooling performance. This can be explained by the same mechanisms mentioned above for the discharge behavior of receivers.

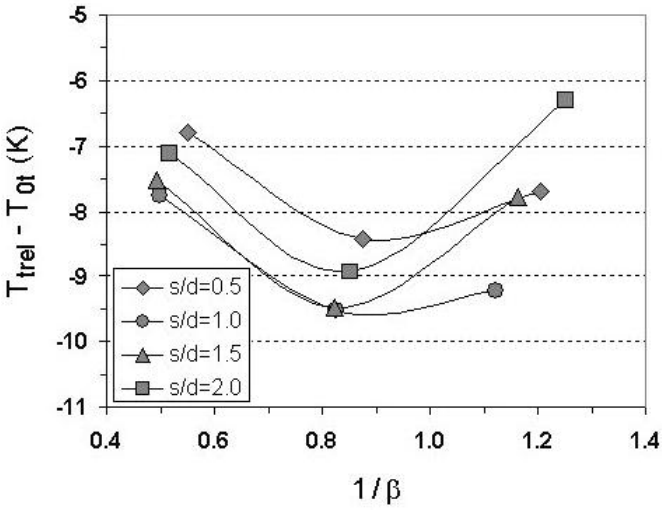

Fig.17. Temperature drop with chamber width.

4 Conclusions

An investigation into the operation characteristics of gas turbine preswirl cooling systems has computationally been performed, using a validated three-dimensional quasi-steady model. In the first phase of the study, the system has been analyzed with respect to different operating conditions. It has been shown that the system operates with the best performance in the vicinity of nominal swirl case. However, for strong over and under swirl operating conditions, the discharge behavior of receivers deteriorates, and the cooling air temperature increases.

In the second phase of the study, system performance has been analyzed as function of the geometry. It was observed that radiusing receiver inlets can improve the performance. It was additionally found out that the receiver length has to be optimized in such a way that the flow can reattach to the walls, on the one side (sufficiently long), but the friction losses remain low, on the other side (but not too long). It was shown that the preswirl chamber should have an optimal width, which balances the effects of high gradients and viscous losses.

Nomenclature

C	absolute velocity (m/s)
C_D	discharge coefficient (-)
c_p	isobaric specific heat (J/kgK)
d	receiver diameter (m)
l	receiver length (m)
$\dot{m}$	mass flow rate (kg/s)
N	rotor speed (rpm)
p	pressure (Pa)
R	gas constant (J/kgK)
r	fillet radius of receiver inlet (m)
s	preswirl chamber width (m)
T	temperature (K)
U	rotor speed at receiver hole radius (m/s)
W	relative velocity (m/s)
y^+	non-dimensional wall distance (-)
α	angle betw. presw. nozzle and swirler plate (rad)
β	swirl ratio (-)
κ	isentropic exponent (-)
Π	pressure ratio (-)

Subscripts

ax	axial
id	ideal
is	isentropic
PSN	Preswirl nozzle
R	receiver hole
real	real
rel	relative
s	static
t	total, tangential
0	domain inlet
1	preswirl outlet
2	domain outlet

References:

[1] Owen, J. M. and Rogers, R. H., Flow and Heat Transfer in Rotating-Disc Systems, Vol. I: Rotor-Stator Systems, Research Studies Press, Taunton; John Wiley, New York, 1989.

[2] Owen, J. M. and Rogers, R. H., Flow and Heat Transfer in Rotating-Disc Systems, Vol. II: Rotating Cavities, Research Studies Press, Taunton; John Wiley, New York, 1995.

[3] Meierhofer, B., and Franklin, C. F., An Investigaton of a Preswirled Cooling Airflow to a Turbine Disc by measuring the Air Temperature in the Rotating Channels, ASME Paper, 81-GT-132, 1981.

[4] Benim, A.C., Nahavandi, A. Stopford, P.J. and Syed, K.J., Modeling Turbulent Swirling Flows in Gas Turbine Combustors with Transient Three-Dimensional Procedures, WSEAS Transactions on Fluid Dynamics, Vol. 1, No.5, 2006, pp. 465-471.

[5] Anagnostopoulos, J.S., CFD Analysis and Design Effects in a Radial Pump Impeller, WSEAS Transactions on Fluid Dynamics, Vol. 1 No.7 2006, pp.763-770.

[6] Djanali, V.S., Wong, K.C. and Armfield, S.W., Numerical Simulations of Transition and Separation on a Small Turbine Cascade, WSEAS Transactions on Fluid Dynamics, 2006, Vol. 1 No.9, pp. 879-884.

[7] Karabay, H., Chen, J. -X., Pilbrow, R., Wilson, M.and Owen, J. M., Flow in a "Cover-Plate" Pre-Swirl Rotor-Stator System, ASME Journal of Turbomachinery, Vol. 121, 1999, pp. 160-166.

[8] Pilbrow, R., Karabay, H., Wilson, M. and Owen, J.M., Heat Transfer in a "Cover-Plate" Pre-Swirl Rotating-Disk System, ASME Journal of Turbomachinery, Vol. 121, 1999, pp. 249-256.

[9] Popp, O., Zimmermann, H., Kutz, J., CFD Analysis of Coverplate Receiver Flow, ASME Journal of Turbomachinery, Vol. 120, 1998, pp. 43-49

[10] Yan, Y., Gord, M. F., Lock, G. D., Wilson, M. and Owen, J. M., Fluid Dynamics of a Pre-Swirl Rotor-Stator System, ASME Journal of Turbomachinery, Vol. 125, 2003, pp. 641-647

[11] Schneider, O., Dohmen, H. J. and Benra, F.-K., Analysis of Dust Separation Inside Pre-Swirl Cooling Air System, ISROMAC10-2004-029, 2004.

[12] Benim, A. C., Brillert, D. and Cagan, M., Investigation into the Computational Analysis of Direct-Transfer Pre-Swirl Systems for Gas Turbine Blade Cooling, ASME Paper GT2004-54151, 2004.

[13] Benim, A. C., Cagan, M., Bricaud, C., Bonhoff, B., Brillert, D., Computational Analysis of Flow and Heat Transfer in a Direct-Transfer Pre-Swirl System, Proceedings of the Sixth European Conference on Turbomachinery – Fluid Dynamics and Thermodynamics, March 7-11, 2005, Lille France, Vol. II, 2005, pp. 864-875.

[14] Benim, A.C., Cagan, M., Bonhoff, B. and Brillert, D., Simulation of Flow in Gas Turbine Pre-Swirl Systems with Emphasis on Rotor-Stator Interface Treatment, Third IASME/WSEAS International Conference on Fluid Mechanics and Aerodynamics, August 20-22, 2005, Corfu, Greece.

[15] Fluent 6.3, User's Guide, Fluent Inc. Lebanon, New Hampshire, 2006.

[16] Vandoormal, J. P. and Raithby, G. D., Enhancements of the SIMPLE Method for Predicting Incompressible Fluid Flows, Numerical Heat Transfer, 7, 1984, pp. 147-163.

[17] Shih, T.-H., Liou, W. W., Shabbir, A. and Zhu, J., A New k-ε Eddy-Viscosity Model for High Reynolds Number Turbulent Flows - Model Development and Validation, Computers and Fluids, 24, 1995, pp. 227-238.

[18] Kim, S.-E., and Choudhury, D., A Near Wall Treatment Using Wall Functions Sensitized to Pressure Gradient, ASME FED Vol. 217 Separated and Complex Flows, 1995.

[19] Barth, T. J. and Jespersen, D., The Design and Application of Upwind Schemes on Unstructured Meshes, Technical Report AIAA-89-0366, 1989.

[20] Benim, A. C. and Arnal. M., A Numerical Analysis of the Labyrinth Seal Flow, in: S. Wagner, E. H. Hirschel, J. Périaux and R. Piva (Eds.), Computational Fluid Dynamics'94, Vol. 2, John Wiley & Sons Ltd., New York, 1994, pp. 839-846.

[21] Dittmann, M., Geis,T., Schramm,V., Kim,S. and Wittig, S., Discharge Coefficients of a Pre-Swirl System in Secondary Air Systems, ASME Journal of Turbomachinery, Vol. 124, 2002, 2002 pp.119-124.

[22] Geis, T., Dittmann and M. and Dullenkopf, K., Cooling Air Temperature Reduction in a Direct Transfer Preswirl System, Journal of Engineering for Gas Turbines and Power, Vol. 126, 2004, pp. 809-815.

[23] Dittmann, M., Dullenkopf, K. and Wittig, S., Discharge Coefficients of Rotating Short Orifices With Radiused and Chamfered Inlets, Journal of Engineering for Gas Turbines and Power, Vol. 126, 2004, pp. 803-808.

[24] Wittig, S., Kim, S., Jakoby, R. and Weissert, I., Experimental and Numerical Study of Orifice Discharge Coefficients in High-Speed Rotating Disks, Journal of Turbomachinery, Vol. 118, 1996, pp. 400-407.